

Received August 24, 2020, accepted October 2, 2020, date of publication October 19, 2020, date of current version November 4, 2020.

Digital Object Identifier 10.1109/ACCESS.2020.3031894

# Tailoring of the Structural and Optoelectronic Properties of Zinc-Tin-Oxide Thin Films via Oxygenation Process for Solar Cell Application

MOHAMMAD AMINUL ISLAM<sup>1,2</sup>, (Member, IEEE),  
MD. KHAN SOBAYEL BIN RAFIQ<sup>3</sup>, (Associate Member, IEEE), HALINA MISRAN<sup>2</sup>,  
MD. AKHTAR UZZAMAN<sup>3</sup>, (Senior Member, IEEE), KUAANAN TECHATO<sup>4</sup>,  
GHULAM MUHAMMAD<sup>5</sup>, (Senior Member, IEEE), AND NOWSHAD AMIN<sup>2,6</sup>

<sup>1</sup>Department of Electrical Engineering, Faculty of Engineering, University of Malaya, Kuala Lumpur 50603, Malaysia

<sup>2</sup>Institute of Sustainable Energy, Universiti Tenaga Nasional (The National Energy University), Kajang 43000, Malaysia

<sup>3</sup>Solar Energy Research Institute, The National University of Malaysia, Bangi 43600, Malaysia

<sup>4</sup>Department of Sustainable Energy, Faculty of Environmental Management, Prince of Songkla University, Songkhla 90110, Thailand

<sup>5</sup>Department of Computer Engineering, College of Computer and Information Sciences, King Saud University, Riyadh 11451, Saudi Arabia

<sup>6</sup>Faculty of Engineering and Built Environment, The National University of Malaysia, Bangi 43600, Malaysia

Corresponding authors: Mohammad Aminul Islam (aminul.islam@um.edu.my) and Nowshad Amin (nowshad@uniten.edu.my)

This work was supported in part by the Institute of Sustainable Energy (ISE), Universiti Tenaga Nasional (The National Energy University), Malaysia, through the BOLD2025 Program, in part by the Researchers Supporting Project, King Saud University, Riyadh, Saudi Arabia, under Grant RSP-2020/34, and in part by the Faculty of Engineering, University of Malaya, Malaysia.

**ABSTRACT** In this study, the impact of compositional variation in high resistance transparent (HRT) metal oxide ZTO films of thickness around 100nm has been investigated. The atomic composition in the films has been tailored by the change of RF power and sub-sequent thermal oxygenation in mixed nitrogen and oxygen atmosphere. A phase transition from  $ZnSnO_3$  to  $ZnSnO_4$  was observed in the X-ray diffraction spectra, indicating the possible oxygen incorporation into the films during the thermal annealing process. Uniform microstructures with compact interconnected grains of around 6-7 nm were found in SEM images while no significant changes been observed upon oxygenation. Besides, the significant alteration of electronic properties was noticed as an effect of compositional variation via oxygenation. All the films showed above 85% of optical transmittance in the visible light spectrum. The optimum optoelectronic properties for RF power has been determined as of 50W ( $ZnO$ ) and 10W ( $SnO_2$ ) via thermal oxygenation at 400°C where the ratio  $O/(Zn+Sn)$  become around 1.6. The significant effect of oxygenation has been realized via primarily fabricated solar cells where the cell with  $ZnSnO_4$ HRT shows higher efficiency than the  $ZnSnO_3$ .

**INDEX TERMS** ZTO thin film, co-sputtering, phase transformation, HRT film, CdTe solar cell.

## I. INTRODUCTION

In recent years, high resistance transparent (HRT) metal oxide compounds have drawn widespread attention for improving the photovoltaic characteristics of thin-film heterostructure solar cells. Particularly, using HRT materials as a buffer layer beneath of the cadmium sulfide (CdS) layers in cadmium telluride (CdTe), copper-indium-gallium-selenide (CIGS), and copper-zinc-tin-sulfide (CZTS) thin-film solar cells can significantly ameliorate the pin-hole problem that is created due to the ultra-thin CdS layer ( $\leq 100$  nm). In general, the ultra-thin CdS layer is being used in these solar cells for

minimizing the considerable absorption by CdS thin film in the blue region [1]–[3]. However, the ultra-thin CdS layer adversely affects the cell efficiency via increasing pin-hole (discontinuity) and locally shorted the absorber material with TCO and front contact, which leads to excessive shunting or unwarranted forward current, and therefore negatively affects the solar cell efficiency [4]. Apart from the reduction of the pin-hole effect, the inclusion of an HRT layer shows improvement on the uniformity and junction quality in a manner parallel to that found for CdTe [5], [6],  $CuInSe_2/CdS$ , and a-Si thin-film cells [7]. Several materials have already been tested for the HRT layer including the  $SnO_2$  [8],  $In_2O_3$  [9],  $TiO_2$  [10],  $Ga_2O_3$  [11], and  $Zn_2SnO_4 / ZnSnO_3$  (ZTO) [12]. Among the aforementioned HRT materials, the ZTO shows

The associate editor coordinating the review of this manuscript and approving it for publication was Padmanabh Thakur<sup>1</sup>.

very promising for solar cell application because of its high carrier mobility (in the range of 5–20 cm<sup>2</sup>/Vs) [13], high optical transmittance (above 80% in the visible region), and admirable resistivity ( $\sim 10$ – $20 \Omega\text{-cm}$ ) [14], [15]. Besides, the optoelectronic properties of ZTO films can also be tailored by changing the atomic ratio of oxygen (O) to tin (Sn) by ensuring a proper stoichiometry of the film. Furthermore, the ZTO has high electron affinity (5.3 eV) for which it catches attention as a hole extracting material in polymer and organic solar cells [16]. Likewise, other than the solar cell application, amorphous ZTO thin films have widely been used for flexible field-effect transistors (FETs) [17] and thin-film transistors (TFTs) [18].

There are two types of ZTO: the spinel-type of Zn<sub>2</sub>SnO<sub>4</sub> and the perovskite-type of ZnSnO<sub>3</sub>. The resistivity of Zn<sub>2</sub>SnO<sub>4</sub> is usually higher than that of ZnSnO<sub>3</sub> [19]. This is reflected well in literature data of conductivity for ITO ( $\sigma = 104 \Omega^{-1}\text{cm}^{-1}$  [20]), for HRT layers as Zn<sub>2</sub>SnO<sub>4</sub> ( $\sigma = 50$ – $100 \Omega^{-1}\text{cm}^{-1}$  [21, 22]) and for ZnSnO<sub>3</sub> ( $\sigma = 250 \Omega^{-1}\text{cm}^{-1}$  [17], [23]). It should be mentioned that the properties of ZTO films are critically dependent on the growth conditions. Amended understanding of ZTO film's structural evolution, surface morphology, optical and electrical properties with its growing conditions are indispensably needed not only for the enrichment of all concurrent practical applications but also for reconnoitering the novel possible technology. The primary objective of the present study is to find out the influence of fabrication parameters, especially the oxygenation process on the structural, morphological, and optoelectronic properties of the co-sputtered ZTO films. It should be noted that the sputtering technique could facilitate precise thickness, chosen elemental composition with a controlled amount of impurity in a long-range, thus, it could be the utmost deposition method for ZTO thin film fabrication.

## II. METHODOLOGY

### A. EXPERIMENTAL DESIGN AND PROCEDURE

ZTO thin films of about 100 nm thickness were deposited by radio frequency (RF) magnetron co-sputtering from ZnO (Plasma Materials 99.999%) and SnO<sub>2</sub> (Plasma Materials 99.999%) targets on commercially available quartz glass substrates. The co-sputtering process is shown schematically in Figure 1(a). The sputtering has been done in Ar ambient with the total pressure to be 8–10 mT, with baseline pressure of  $10^{-2}$  mT. The films were deposited at 300°C of substrate temperature using deposition RF power of 50 watts for ZnO, and 05 watts and 10 watts for SnO<sub>2</sub> target. The deposition power in the SnO<sub>2</sub> target was varied to obtain the film with different Zn/Sn ratios. The extra oxygen was induced in the films via thermal annealing in N<sub>2</sub> and O<sub>2</sub> ambient with ratio (80:20) at two high temperatures 400°C and 500°C for 30 minutes. A simple quartz tube has been used for the oxygenation process as shown schematically in Figure 1(b) which has a gas inlet, a vacuum outlet, two electrical coils (one on top and another at the bottom), each of 2 kW.

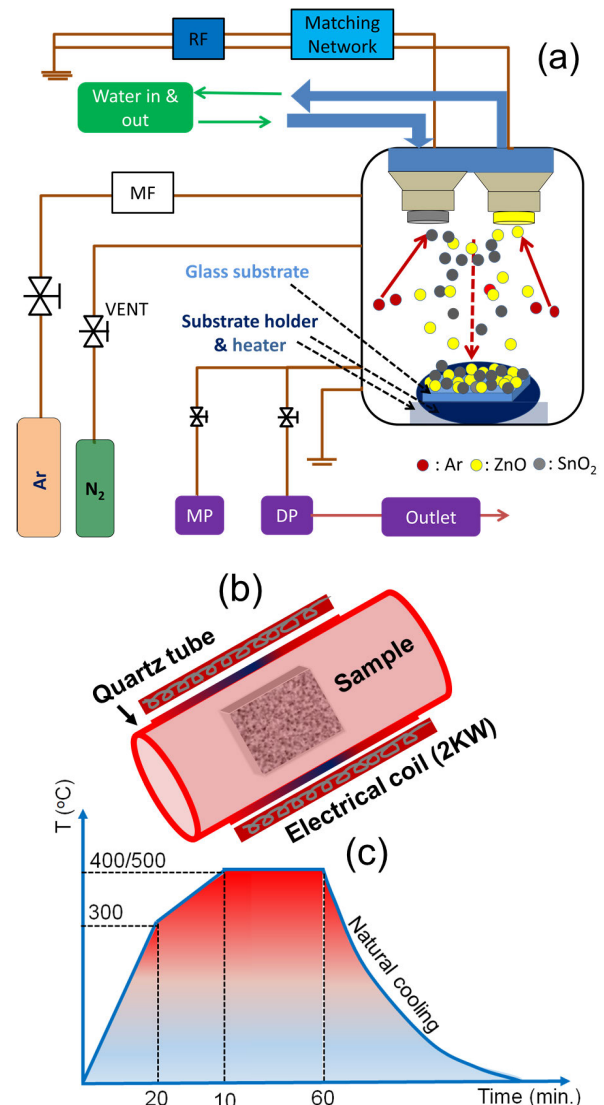


**FIGURE 1.** (a) Schematic diagram of the co-sputtering process, (b) Schematic diagram of the thermal annealing process, and (c) thermal annealing profil.

### B. CHARACTERIZATION

X-ray diffraction (XRD) spectroscopy ('BRUKER aXS-D8 Advance Cu- K $\alpha$ ) has been employed for investigating the structural variation in the films. The surface morphology of the films was observed from the FESEM images carried out by 'LEO 1450 Vp'. Electronic properties including carrier mobility, concentration, and resistivity of the films were measured using the Hall-Effect measurement system 'ECOPIA 3000'. The film transmittance, absorbance, and optical bandgap were measured by using Perkin Elmer Instruments Lambda35 UV-vis spectrometry.

The complete solar cells have been primarily fabricated using ZTO thin films as HRT material that deposited on top of the commercial fluorine-doped tin oxide (FTO) coated glass substrates. The subsequent CdS and CdTe thin films have also been fabricated on top of the FTO/ZTO stacks. The cell fabrication was completed using

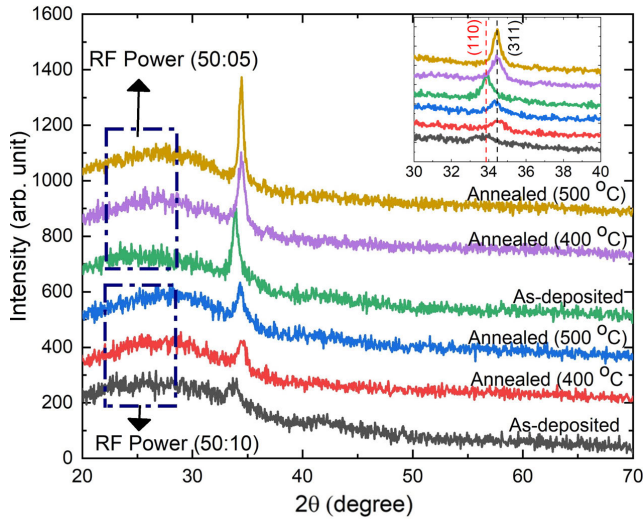


**FIGURE 2.** XRD diffraction spectra of co-sputtered ZTO thin films prepared using different RF power and subsequent oxygenation in  $N_2/O_2$  ambient (peaks are assigned by JCPDS No. 010890095 for  $ZnSnO_3$  and 010731725 for  $Zn_2SnO_4$ ).

C: Cu/Ag back contact. Before fabricating the back-contact, the Glass/FTO/ZTO/CdS/CdTe stacks were  $CdCl_2$  treated for achieving Te rich surface. The printed paste was prepared by 3 gm of Cu powder adding to the 10 gm of commercial Carbon paste and mixed them for 1 h. using a rotating magnet. The C: Cu printed layers were dried for 30 min at a temperature of 120 °C in an oven. After that, the completed cells were annealed for 15 min in a vacuum furnace at 500 mT of  $N_2$  pressure and temperature of 260 °C. During the vacuum annealing, Cu supposed to be diffused and expecting to be formed an ultra-thin  $Cu_xTe$  layer on the CdTe surface. Finally, device fabrication was completed by printing Ag as a second electrode. The performance of the cell with an area of 25  $mm^2$  was evaluated under standard illumination (1.5 AM) employing ‘Gratings Inc. Solar Cell Tester: VI & power management system’.

### III. RESULTS AND DISCUSSION

#### A. STRUCTURAL ANALYSIS

The XRD analysis was performed to investigate the crystallographic growths including crystallinity and crystal phases of the prepared ZTO films as shown in Figure 2. The broad peaks with very low intensity indicating poor crystallinity. On the other hand, there is a peak shift from (110) of  $ZnSnO_3$  (JCPDF, card no. 24-1470) to (311) of  $Zn_2SnO_4$  (JCPDS file No: 01-074-2184) has been observed due to the annealing in an oxygen ambient. Peak shifting confirms that additional oxygen atoms have been incorporated into the ZTO lattice during the annealing and shifting occurred to the higher angle because the oxygen ions ( $O^{2-}$ ) have smaller radii than  $Zn^{2+}$  ions and  $Sn^{4+}$  ions. Also, due to the smaller ionic radii, the oxygen ions easily substitute the Zn and/or Sn ions. Similar phenomena could also occur if Zn ions are replaced by Sn ions [24]. It has been identified that the amorphous structure of ZTO is dominant instead of a crystalline

**TABLE 1.** Estimated structural properties of the co-sputtered ZTO thin films and subsequent oxygenation via thermal annealing in  $N_2/O_2$  ambient.

RF Power (W)	Sample ID	$2\theta$ ( $^\circ$ )	Plane (hkl)	I (a.u.)	D (nm)	$\epsilon$ ( $\times 10^{-3}$ )	$\delta$ ( $\times 10^{15} cm^{-2}$ )
ZnO/SnO <sub>2</sub> = 50/05	As-dep.	33.86	(110)	352	10.79	11.03	8.59
	Ann. 400 °C	34.71	(311)	339	11.18	10.39	8.01
	Ann. 500 °C	34.52	(311)	369	11.98	9.75	6.97
ZnO/SnO <sub>2</sub> = 50/10	As-dep.	33.82	(110)	150	10.25	11.62	9.50
	Ann. 400 °C	34.56	(311)	195	10.81	10.79	8.55
	Ann. 500 °C	34.56	(311)	233	11.56	10.09	7.48

structure [25] and it could be crystalline if only Zn/Sn ratios become close to 2.0, at a temperature above 500°C [26]. Alternatively, Rajachidambaram *et al.* [27] found that the ZTO films retain its amorphous nature even it is annealed at 600 °C. Particularly, the integration of excess elements, such as Sn, In, Ga, or Al, etc. into the ZnO matrix tempts the alteration into the amorphous form instead of the crystalline phase [28], [29]. Thus, the ZTO films prepared in low RF power of SnO<sub>2</sub> which certainly have low Sn concentration are showing higher peak intensity than the high RF power as seen in the peak intensity values (Table 1). The crystallite size (D) of the films was estimated using the well-known Scherer’s formula [30].

The poor crystalline nature as seen in Figure 2 implies that films belong to a higher number of lattice misfit and lattice strain. It is known that the lattice strains could be developed in the films via scattered grains distribution and/or relocation of the atoms from their reference-lattice positions. However, these phenomena are in turn depends on the films’ predation conditions including deposition parameters and sub-sequent annealing conditions. Simply, the lattice strain that developed in the film can be known by estimating “micro-strain”. Alternatively, the atoms that displace from its reference lattice could act as interstitial atoms and its reference place could act as an unlike vacancy in the crystals. The number of atoms that displaced from their reference lattice could be realized via estimating the dislocation density.

The micro-strain ( $\epsilon$ ) and dislocation density ( $\delta$ ) that indicate the defectiveness of a crystal associated with mis-registry of the lattices and atoms could be calculated using the following equations [30]:

$$\epsilon = \frac{\beta}{4\tan\theta} \tag{1}$$

And

$$\delta = \frac{1}{D^2} \tag{2}$$

where  $\theta$ ,  $\beta$ , and D have their usual significances as mentioned in the above section. All the estimated values, such as D,  $\epsilon$ , and  $\delta$  for ZTO thin films are tabulated in Table 1 and compared concerning the RF power and subsequent

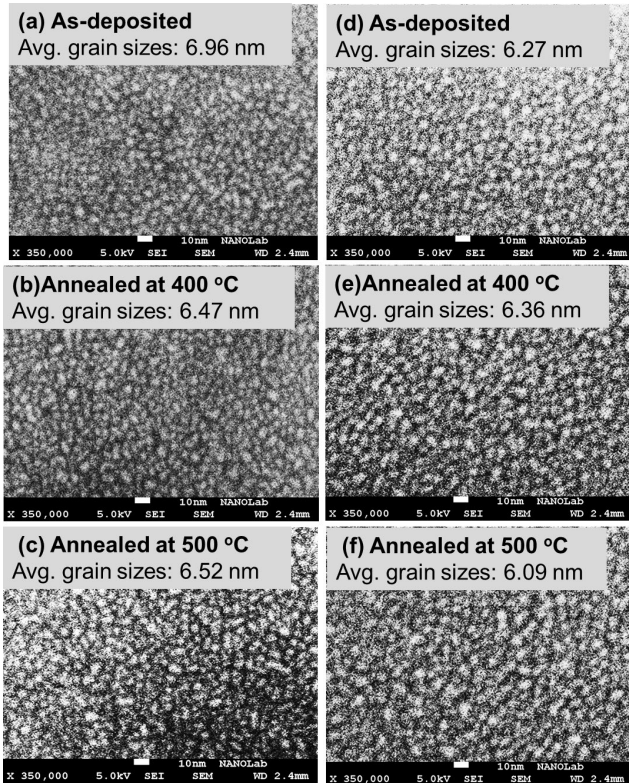


**FIGURE 3.** FESEM images of ZTO thin films deposited in Ar ambient and subsequent oxygenation in  $N_2:O_2$  ambient, (a)-(c) for RF power of ZnO/SnO<sub>2</sub> (50/05W) and (d)-(e) for RF power of ZnO/SnO<sub>2</sub> (50/10W) (average grain size has been estimated by ImageJ software).

annealing temperature. It could be seen in Table 1 that the values D of the ZTO films are increased with the increase of annealing time. The micro-strain of the films is found very high, which does not show any significant change by annealing temperature may be due to lack of enough energy supply during annealing that is needed for reconstructing the grains. However, dislocation densities are abridged as the increase of annealing temperature suggests that the interstitial defects which lead to lattice misfit and/or dislocation are reduced in the film by annealing. Overall, the lowest micro-strain, which is the indicator of lattice misfits, is found for 5 watts of SnO<sub>2</sub> film after annealing at 500°C stipulated the strains are released at this temperature comparatively higher than other films.

### B. EVALUATING MORPHOLOGICAL & OPTICAL PROPERTIES OF FILM

Films' surface morphology has been investigated via FESEM images as shown in Figure 3. The surface of the films is found dense with nano-platelets; shows very tinny nano-structured; and spherical shaped grains are well distributed over the entire substrate surface. The film's average grain sizes have been estimated by employing ImageJ software [31] and could be seen in Figure 3 that the grain size is decreased slightly with the increase of SnO<sub>2</sub> deposition power. The average grain size of the films deposited at RF power of

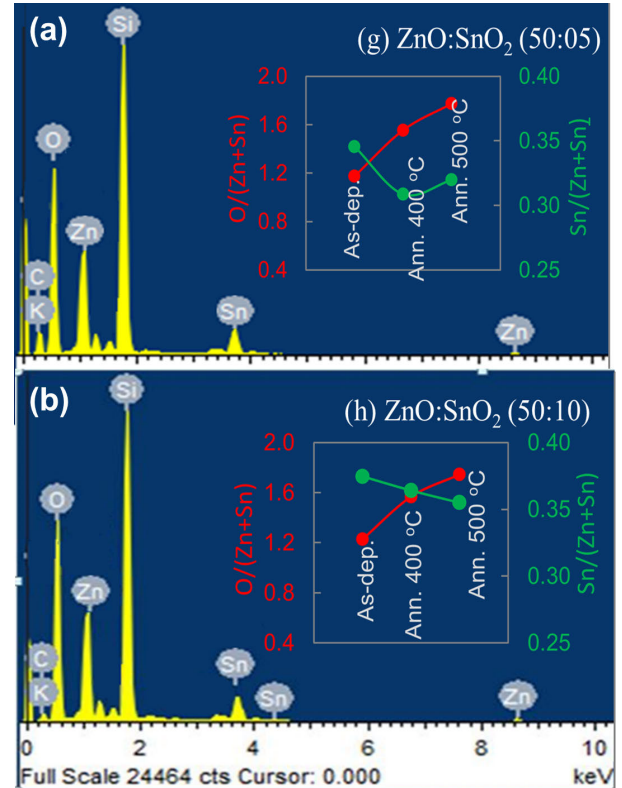


**FIGURE 4.** (a) and (b) EDX spectra of the film that was at annealed at 500°C in mixed  $N_2:O_2$  ambient (inset figure shows the difference of elemental compositions and the lines are drawn for guiding the eyes).

ZnO/SnO<sub>2</sub> (50/05W) is 6.65 nm and the RF power of ZnO/SnO<sub>2</sub> (50/05W) is 6.24 nm. The compositional analysis as shown in Figure 4(a) and 4(b) were corroborated by the EDX result, which for only the films annealed at 500°C. The EDX spectrum confirmed the presence of Zn, Sn, and O elements in the prepared films. The films' elemental compositions could be seen in the insight of Figure 4(a) and 4(b) presented in ratios of Sn/(Zn+Sn) and O/(Zn+Sn) for all films. It could be seen that the atomic concentration of Sn is reduced where O is increased with the increase of annealing temperature that leads to the variation of the optoelectronic properties discussed in the next section. The initial atomic ratio of O with the sum of Zn and Sn is about to 1.2, which increased about to 1.8 upon thermal oxygenation. As the concentration of O is increased, the film's crystal phase changed from ZnSnO<sub>3</sub> to ZnSnO<sub>4</sub> as seen in XRD. Besides, the Si, K, and C signals have also appeared from the substrate and the trace elements.

Optical transmittance curves of ZTO films deposited by different RF power and subsequent annealing are shown in Figure 5(a) and 5(b). All the films secured an admirable optical transmittance of above 85% in the range of 400 to 900 nm which is a vital need for using a thin film as an HRT buffer layer in thin-film heterojunction solar cells. Moreover, the transmittance increases in the shorter wavelength region (blue shift) is seen for all the annealed films that may be related to the oxygen incorporation into the films.

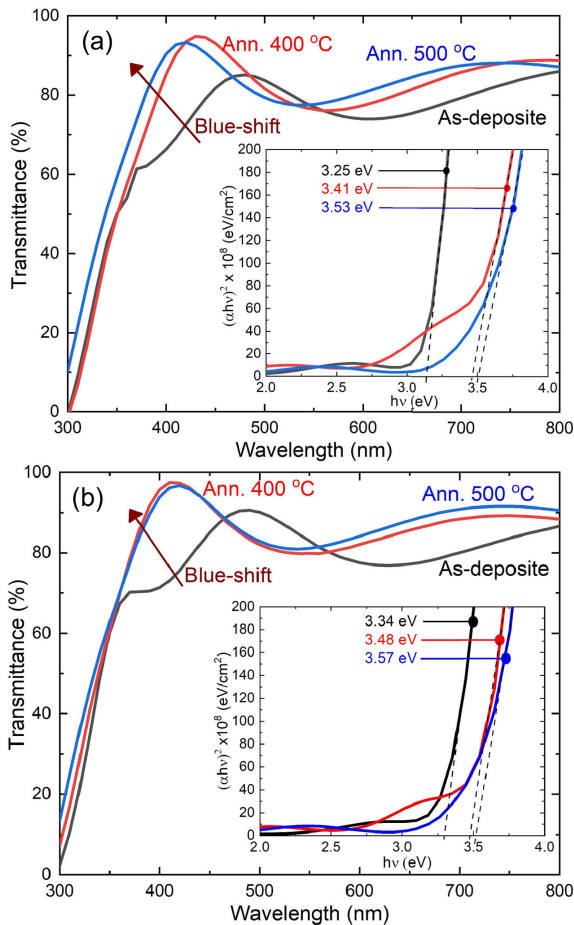


**FIGURE 5.** Transmittance curves of co-sputtered and annealed ZTO thin films, (a) for RF power of ZnO: SnO<sub>2</sub> (50/05W) and (b) for RF power of ZnO: SnO<sub>2</sub> (50/10W) (inset: bandgap evaluation curves for the corresponding films).

Inset of Figures 5(a) and 5(b) depict the  $h\nu$  vs.  $(\alpha h\nu)^2$  plots enabling the  $E_g$  to be determined [32]. Comparing with the EDX composition represent in the previous section, it could be realized that the bandgap is increased by the decrease of Sn concentration as well as by the increase of O concentration availed during the post-deposition thermal annealing. It is well known that the bandgap is oppositely changed with the grain size in the case of thin films, this study also shows similar results as compared to SEM images with the films' bandgap. In this case, the elemental composition certainly played a domineering role. The variation of the bandgap may also be corresponding to the film's crystallographic variations as seen in Figure 2. The bandgap found in this study is ranging from 3.25 eV to 3.57 eV which is consistent with the previous study published elsewhere [22], [33].

**C. INVESTIGATION ON ELECTRICAL PROPERTIES**

The electronic properties of the films were investigated by employing the Hall-Effects measurement system as shown in Table 2. It could be seen that the resistivity of the films increased with the increase of annealing or oxygenation temperature. Alternatively, the resistivity increased with the

**TABLE 2.** Resistivity, mobility, and carrier concentration of ZTO thin films deposited via different RF power of ZnO and SnO<sub>2</sub> and subsequent oxygenation via thermal annealing in N<sub>2</sub>: O<sub>2</sub> ambient.

RF power (ZnO/SnO <sub>2</sub> )	Film condition	Resistivity (Ω-cm)	Mobility (cm <sup>2</sup> /V-S)	Carrier conc. (×10 <sup>16</sup> cm <sup>-3</sup> )
50W/05W	As-dep.	4.32	16.5	8.5
	400°C	21.2	17.9	1.7
	500°C	49.1	10.8	1.2
50W/10W	As-dep.	2.06	17.5	15.1
	400°C	4.42	19.7	7.9
	500°C	12.2	14.3	3.8

increase of O and Zn atomic concentration. The highest resistivity of 48.1 Ω-cm is seen for the annealed (500°C) film of RF power 50/05W and the minimum resistivity of 2.06 Ω-cm is seen for the as-deposited film of RF power 50/10W. This radical change of resistivity is suspected due to the increase of O atoms and reduction of Sn atoms in the film as could be seen in Figure 4(a) and 4(b). However, it is seen that the film's resistivity is directly correlated (inversely varied) with the change of carrier concentration. It was reported that the relatively low carrier concentrations and/or high resistivity are linked to the carrier conduction led by grain boundary scattering that developed by enrichment of oxygen atoms into the films and/or oxygen adsorption onto the grain-boundary of the films [34], [35]. In general, the carrier concentration could be improved by the oxygen-vacancy creation in ZTO thin films via annealing under an oxygen-free ambient [36], however, it is difficult to precisely control the carrier concentrations by oxygen reduction process because it is highly sensitive to process conditions. Besides, carrier concentration could also be improved by the increase of Sn concentration, since valence electrons of Sn and Zn are four and two, thus, Sn could donate two extra electrons when it substituting the Zn atoms or occupying an interstitial site [36].

In the case of semiconductors thin films, carrier concentration, and mobility are considered two key factors that control the carrier transport properties. The significant impact of RF power and subsequent annealing temperature on carrier mobility has been observed. The best mobility as high as 20–50 cm<sup>2</sup>/Vs have been reported so far for the film deposited by sputtering and post-annealed at 600°C [25]. In this study, carrier mobility is found to be in the range of 10.8 cm<sup>2</sup>/Vs to 19.7 cm<sup>2</sup>/Vs and the utmost mobility is attained for the film of RF power 50/10W after 400°C of thermal annealing in an oxygen ambient. It should be noted that the mobility is somehow affected by the deposition condition as it was reported for ZnO thin films grown by sputtering technique [37]. However, the variation of the mobility due to the thermal oxygenation indicating the level of defect density in the films. As the films of the highest O concentration show low mobility, thus, it is reasonably possible that grain boundary scattering is dominated in the carrier conduction in this case as we mentioned earlier. Also, the simultaneous reduction of carrier concentration and mobility in some films suggesting the ionized defect density including sub-bandgap defect density might increase as an impact of thermal annealing [38].

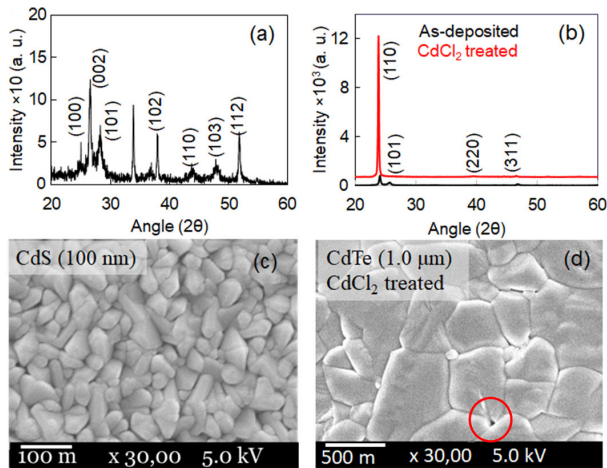


**FIGURE 6.** XRD spectrum of (a) CdS thin film and (b) CdTe thin-film XRD and FESEM image of (c) CdS and (d) CdTe thin film (marked red circle show the pinhole in the CdTe thin film).

The above analysis clarifies that the film composition and subsequent annealing have a crucial role in film electronic properties, certainly, that brought a great impact on the performance of thin-film solar cells.

**D. EVALUATION ON SOLAR CELL PERFORMANCE**

Complete solar cells have been primarily fabricated for investigating the effect of ZTO film as an HRT on solar cell performance. For completing the solar cell, the CdS and CdTe thin films have been prepared by sputtering technique at a growth rate of 1.8 Å/s, and 4.6 Å/s, respectively on top of “glass/FTO/ZTO” stacks. Both films were deposited using a substrate temperature of 300 °C and a working pressure of 14 mT. The film thickness of CdS is about to 100 nm and CdTe is about to 2.0 μm. The crystallographic and surface properties of the CdS and CdTe thin films including CdCl<sub>2</sub> treated CdTe thin film are shown by XRD and SEM images (Figure 6). XRD spectra show poly-crystalline CdS and CdTe film with preferential orientation (220) and (110), respectively. The crystallinity of CdTe has significantly changed after the CdCl<sub>2</sub> treatment, which has been performed by dipping the FTO/ZTO/CdS/CdTe stacks on to the 0.3 M of CdCl<sub>2</sub> solution and subsequent vacuum annealing at 390°C for 15 min. Readers are referred to our previous publication regarding the details of the CdCl<sub>2</sub> treatment [2]. The inhomogeneous grains with an average grain size of 100 nm are mainly observed in the FESEM image of CdS. The uniformly distributed grains are covered the whole surface homogeneously and no pinholes and/or cracks are observed. Instead, the average grain CdTe thin-film after treated by CdCl<sub>2</sub> is about to 700 nm, however, some tiny holes are observed as marked in the FESEM image that may affect the cell performance.

The schematic structure of FTO/ZTO/CdS/CdTe/C: Cu/Ag solar cell is shown in the inset of Figure 7(a). The light J-V characteristics of the solar cells are shown in Figure 7(a) and the performance parameters of individual solar cells are shown in Table 3. Diode ideality factor (n), saturation current

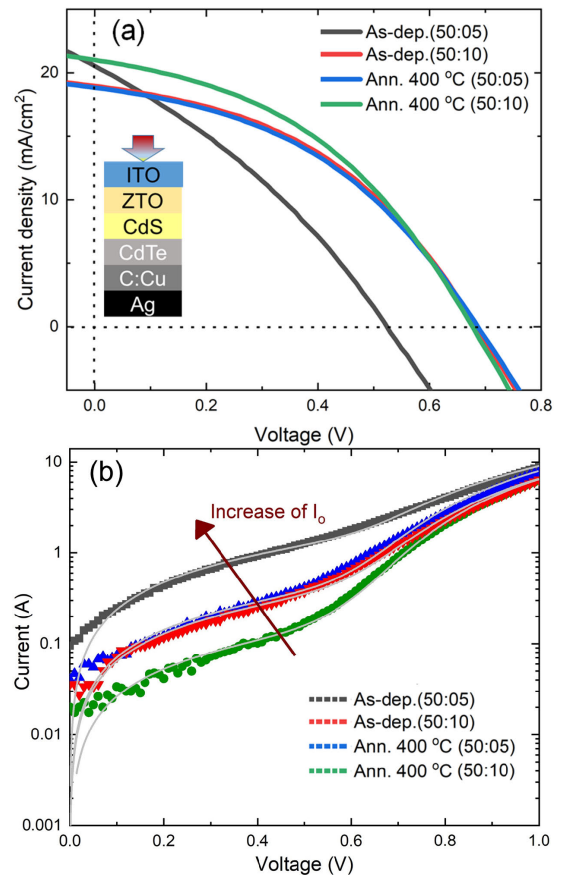


**FIGURE 7.** (a) Light J-V curve and (b) dark I-V curves in the semi-log mode for FTO/ZTO/CdS/CdTe/C: Cu/Ag solar cells.

**TABLE 3.** Characteristic parameters of the CdS/CdTe solar cells using ZTO as an HRT buffer layer and C: Cu/Ag printed back contact.

Deposition condition	Jsc (mA/cm <sup>2</sup> )	Voc (V)	FF (%)	η (%)	I <sub>0</sub> (×10 <sup>-9</sup> , mA/cm <sup>2</sup> )	n	R <sub>s</sub> (Ω-cm <sup>2</sup> )	R <sub>sh</sub> (Ω-cm <sup>2</sup> )
As-dep. (50/05)	20.54	0.53	35	3.81	13.36	2.39	321	152
As-dep.(50/10)	19.79	0.69	46	6.28	3.91	2.18	314	238
Ann. 400 °C (50/05)	19.83	0.69	46	6.29	5.08	2.25	336	318
Ann. 400 °C (50/10)	21.02	0.67	49	6.90	1.97	1.83	291	378

density (I<sub>0</sub>), shunt (R<sub>sh</sub>), and series resistance (R<sub>s</sub>) have been extracted by the fitting of dark I-V curves as shown in Figure 7(b) using the following diode equation [39].

$$I(V) = I_0 \left[ \exp \left( \frac{q(V - IR_s)}{nkT} \right) - 1 \right] + \frac{V - IR_s}{R_{sh}} \quad (3)$$

where, q is the elementary charge, k the Boltzmann constant, and T the absolute temperature (300 K). I<sub>0</sub>, R<sub>sh</sub>, and R<sub>s</sub> were positive, and n was limited to greater than one. The diode fitting was performed using the OriginPro2015J. The estimated parameters are also shown in Table 3.

It could be seen that all the solar cells showed low open-circuit voltage (V<sub>oc</sub>) and fill factor (FF), which may be attributed to the low R<sub>sh</sub> that was found in the dark I-V analysis as shown in Table 3. It has been seen in SEM image that CdTe films have very tiny pin-hole which may contribute to the low shunt resistance. Other causes of low shunt resistance

may be related to the Cu migration through the CdTe grain boundaries to the depletion region which is considered a very critical issue for fabricating ultra-thin ( $\approx 2.0 \mu\text{m}$ ) CdTe solar cells. Particularly, higher efficiency in CdTe based solar cells achieved for CdTe thickness of above  $5.0 \mu\text{m}$  [31]. Although the  $R_{\text{sh}}$  has improved for the annealed ZTO films, however, the cell FF, as well as efficiencies, were not found in the adequate range, owing to the high  $R_{\text{s}}$  may be associated with the ZTO HRT layer at the front contact. The thickness of the ZTO film is around 100 nm in this study, we believe that reducing the ZTO thickness certainly improve cell performance. Moreover, the bulk resistance of the CdS and CdTe layers and back contact resistance could also contribute to the increase of series resistance. The high saturation current density ( $I_0$ ) has also been observed for all the solar cells indicates significant recombination occurred via defect levels where a large number of defects existed within the depletion region that increase due to the Cu ions migration. The high defect density in the depletion region is a cause for low  $V_{\text{oc}}$ .

The highest value of  $I_0$  is  $13.36 \times 10^{-9} \text{ mA/cm}^2$  has been found for as-deposited ZTO film of RF power of 50/05 W. Alternatively, the lowest  $I_0$  has observed for the ZTO film of RF power 50/10W that was annealed at  $400^\circ\text{C}$ . It should be noted that  $I_0$  in a solar cell is highly dependent on the generation and recombination of charge carriers in the space-charge region [39]. Particularly, decreasing the structural defect density could lead to a decrease of defect density, thus decreasing the recombination current in the depletion region and  $I_0$  in the device [40]. In the case of CdTe devices, the device properties are dominated by recombination at the CdS/CdTe interface which in general has higher defect density due to the large lattice mismatch. However, it could be observed from Table 3 that the ZTO/CdS interface played an important role along with the CdS/CdTe interface which influences the device properties including  $I_0$ . Thus, the lowest  $I_0$  has been observed for the film that has the best crystal properties, highest mobility, and/or lowest defect density. Moreover, the ZTO buffer layer may influence the properties of CdS emitter and CdTe absorber films, as it has been reported that the ZTO buffer layer is promoted to increase the grain size of perovskite films [41].

It is evident that higher efficiency could be achieved by employing the ZTO HRT buffer layer but essential to optimize the FTO/ZTO bilayer properties in the front contact as well as C: Cu/Ag screen printed back contact to create effective ohmic contact for the CdTe solar cells. As a whole, the maximum conversion efficiency of 6.90% has been achieved for the ZTO film of RF power 50/10W that annealed at  $400^\circ\text{C}$  including the performance parameters of  $J_{\text{sc}}$  of  $21.02 \text{ mA/cm}^2$ ,  $V_{\text{oc}}$  of 0.67 V, and FF of 49%.

#### IV. CONCLUSION

We demonstrated extensively the impact of elemental composition on properties of Zn-Tin-Oxide (ZTO) thin films that have been tailored by RF power in the co-sputtering technique and subsequent thermal oxygenation. The oxygenated

films showed better crystallinity with a phase transformation from  $\text{Zn}_2\text{SnO}_3$  to  $\text{Zn}_2\text{SnO}_4$ , however, there has no significant effect been observed in the mean crystallite size, dislocation density, and micro-strain for as-deposited and oxygenated films. All the films showed uniform nanostructure with well-distributed grains that reduce by an increase of  $\text{SnO}_2$ 's deposition power as well as oxygenation temperature. The optical transmission of the films has been found higher than 85% in the visible region and blue-shift is observed in the oxygenated films. The bandgap increases with the increase of O concentration and oxygenation temperature as well. The significant effect of Sn and O concentration on electronic properties has been observed whereby the carrier mobility was found as high as  $19.7 \text{ cm}^2/\text{Vs}$ . The electronic properties of the films are seemed to be affected by the grain boundary scattering that is developed by enrichment of oxygen atoms into the films and/or oxygen adsorption onto the grain-boundary of the films due to the oxygenation. In this study, the optimum optoelectronic properties found for RF power of 50W ( $\text{ZnO}$ ) and 10W ( $\text{SnO}_2$ ) via thermal oxygenation at  $400^\circ\text{C}$  where the ratio  $\text{O}/(\text{Zn}+\text{Sn})$  become around 1.6. The complete solar cells with a novel structure of FTO/ZTO/CdS/CdTe/C: Cu/Ag have been fabricated and as high as 6.9% conversion efficiency was achieved so far. Although, the cells are suffered from the low shunt and high series resistance including very high recombination current, however, the significant effect of oxygenation has already been realized as the cell with oxygenated film ( $\text{ZnSnO}_4$ ) showed higher efficiency than the cell with as-deposited ( $\text{ZnSnO}_3$ ) film. The findings urge the importance of the optimization of ZTO thin films including CdS and CdTe layers for achieving higher efficiency in the ultra-thin solar cell.

#### REFERENCES

- [1] A. Kerimova, E. Bagiyev, E. Aliyeva, and A. Bayramov, "Nanostructured CdS thin films deposited by spray pyrolysis method," *Phys. Status Solidi C*, vol. 14, no. 6, p. 1600144, Jun. 2017.
- [2] M. A. Islam, K. S. Rahman, K. Sobayel, T. Enam, A. M. Ali, M. Zaman, M. Akhtaruzzaman, and N. Amin, "Fabrication of high efficiency sputtered CdS:O/CdTe thin film solar cells from window/absorber layer growth optimization in magnetron sputtering," *Sol. Energy Mater. Sol. Cells*, vol. 172, pp. 384–393, Dec. 2017.
- [3] G. Kartopu, D. Turkay, C. Ozcan, W. Hadibrata, P. Aurang, S. Yerci, H. E. Unalan, V. Barrioz, Y. Qu, L. Bowen, A. K. Gürelek, P. Maiello, R. Turan, and S. J. C. Irvine, "Photovoltaic performance of CdS/CdTe junctions on ZnO nanorod arrays," *Sol. Energy Mater. Sol. Cells*, vol. 176, pp. 100–108, Mar. 2018.
- [4] K. Sarkar and K. K. Ghosh, "Effect of pinhole and its recovery in CdS/CdTe solar cell through fabrication simulation," *Nanomaterials Energy*, vol. 8, no. 2, pp. 178–185, Dec. 2019.
- [5] C. S. Ferekides, R. Mamazza, U. Balasubramanian, and D. L. Morel, "Transparent conductors and buffer layers for CdTe solar cells," *Thin Solid Films*, vols. 480–481, pp. 224–229, Jun. 2005.
- [6] A. Klein, "Energy band alignment in chalcogenide thin film solar cells from photoelectron spectroscopy," *J. Phys. Condens. Matter*, vol. 27, pp. 1–24, Mar. 2015.
- [7] N. Bernhard, G. H. Bauer, and W. H. Bloss, "Bandgap engineering of amorphous semiconductors for solar cell applications," *Prog. Photovoltaics, Res. Appl.*, vol. 3, no. 3, pp. 149–176, 1995.
- [8] T. Baines, G. Zoppi, L. Bowen, T. P. Shalvey, S. Mariotti, K. Durose, and J. D. Major, "Incorporation of CdSe layers into CdTe thin film solar cells," *Sol. Energy Mater. Sol. Cells*, vol. 180, pp. 196–204, Jun. 2018.

- [9] T. Takamoto, T. Agui, H. Kurita, and M. Ohmori, "Improved junction formation procedure for low temperature deposited solar cells," *Sol. Energy Mater. Sol. Cells*, vol. 49, nos. 1–4, pp. 219–225, Dec. 1997.
- [10] E. Hernández-Rodríguez, V. Rejón, R. Mis-Fernández, and J. L. Peña, "Application of sputtered TiO<sub>2</sub> thin films as HRT buffer layer for high efficiency CdS/CdTe solar cells," *Sol. Energy*, vol. 132, pp. 64–72, Jul. 2016.
- [11] T. Koida, Y. Kamikawa-Shimizu, A. Yamada, H. Shibata, and S. Niki, "Cu(In,Ga)Se<sub>2</sub> solar cells with amorphous oxide semiconducting buffer layers," *IEEE J. Photovolt.*, vol. 5, no. 3, pp. 956–961, May 2015.
- [12] C. Doroody, K. S. Rahman, H. N. Rosly, M. N. Harif, F. Haque, S. K. Tiong, and N. Amin, "Impact of high resistivity transparent (HRT) layer in cadmium telluride solar cells from numerical simulation," *J. Renew. Sustain. Energy*, vol. 12, no. 2, Mar. 2020, Art. no. 023702.
- [13] Z. Chen, D. Han, X. Zhang, and Y. Wang, "Improving performance of Tin-Doped-Zinc-Oxide thin-film transistors by optimizing channel structure," *Sci. Rep.*, vol. 9, no. 1, pp. 1–8, Dec. 2019.
- [14] M. K. Jayaraj, J. S. Kachirayil, N. Kenji, T. Kamiya, and H. Hosono, "Optical and electrical properties of amorphous zinc tin oxide thin films examined for thin film transistor application," *J. Vac. Sci. Technol. B, Microelectron. Nanometer Struct. Process., Meas., Phenomena*, vol. 26, pp. 495–501, Mar. 2008.
- [15] M. J. Wahila, Z. W. Lebens-Higgins, K. T. Butler, D. Fritsch, R. E. Treharne, R. G. Palgrave, J. C. Woicik, B. J. Morgan, A. Walsh, and L. F. J. Piper, "Accelerated optimization of transparent, amorphous zinc-tin-oxide thin films for optoelectronic applications," *APL Mater.*, vol. 7, no. 2, Feb. 2019, Art. no. 022509.
- [16] L. Yu, D. Luo, H. Wang, T. Zou, L. Luo, Z. Qiao, Y. Yang, J. Zhao, T. He, Z. Liu, and Z.-H. Lu, "Highly conductive Zinc-Tin-Oxide buffer layer for inverted polymer solar cells," *Organic Electron.*, vol. 33, pp. 156–163, Jun. 2016.
- [17] C. Fernandes, A. Santa, Â. Santos, P. Bahubalindruni, J. Deuermeier, R. Martins, E. Fortunato, and P. Barquinha, "A sustainable approach to flexible electronics with zinc-tin oxide thin-film transistors," *Adv. Electron. Mater.*, vol. 4, no. 7, Jul. 2018, Art. no. 1800032.
- [18] Y.-C. Chen and Y.-R. Shen, "Growth and dielectric characterizations of zinc stannate thin films deposited by RF magnetron sputtering," *Integr. Ferroelectr.*, vol. 192, no. 1, pp. 80–87, Sep. 2018.
- [19] S. Sun and S. Liang, "Morphological zinc stannate: Synthesis, fundamental properties and applications," *J. Mater. Chem. A*, vol. 5, no. 39, pp. 20534–20560, 2017.
- [20] P. H. Le and C. W. Luo, "Nanostructuring indium-tin-oxide thin films by femtosecond laser processing," in *Methods for Film Synthesis and Coating Procedures*. Rijeka, Croatia: InTech, Dec. 2018.
- [21] R. A. Mereu, A. Le Donne, S. Trabattoni, M. Acciarri, and S. Binetti, "Comparative study on structural, morphological and optical properties of Zn<sub>2</sub>SnO<sub>4</sub> thin films prepared by r.f. sputtering using Zn and Sn metal targets and ZnO–SnO<sub>2</sub> ceramic target," *J. Alloys Compounds*, vol. 626, pp. 112–117, Mar. 2015.
- [22] N.-E. Sung, H. J. Shin, K. H. Chae, S. O. Won, and I.-J. Lee, "Epitaxial zinc stannate (Zn<sub>2</sub>SnO<sub>4</sub>) thin film for solar cells," *ACS Appl. Energy Mater.*, vol. 3, no. 7, pp. 6056–6059, Jul. 2020.
- [23] S. Cai, Y. Li, X. Chen, Y. Ma, X. Liu, and Y. He, "Optical and electrical properties of ta-doped ZnSnO<sub>3</sub> transparent conducting films by sol–gel," *J. Mater. Sci., Mater. Electron.*, vol. 27, no. 6, pp. 6166–6174, Jun. 2016.
- [24] C.-Y. Tsay, H.-C. Cheng, Y.-T. Tung, W.-H. Tuan, and C.-K. Lin, "Effect of Sn-doped on microstructural and optical properties of ZnO thin films deposited by sol–gel method," *Thin Solid Films*, vol. 517, no. 3, pp. 1032–1036, Dec. 2008.
- [25] H. Q. Chiang, J. F. Wager, R. L. Hoffman, J. Jeong, and D. A. Keszler, "High mobility transparent thin-film transistors with amorphous zinc tin oxide channel layer," *Appl. Phys. Lett.*, vol. 86, no. 1, Jan. 2005, Art. no. 013503.
- [26] M. A. Patil, S. H. Mujawar, V. V. Ganbavle, K. Y. Rajpure, and H. P. Deshmukh, "Synthesis and characterization of zinc stannate thin films prepared by spray pyrolysis technique," *J. Mater. Sci., Mater. Electron.*, vol. 27, no. 12, p. 12323, 2016.
- [27] J. S. Rajachidambaram, S. Sanghavi, P. Nachimuthu, V. Shutthanandan, T. Varga, B. Flynn, S. Thevuthasan, and G. S. Herman, "Characterization of amorphous zinc tin oxide semiconductors," *J. Mater. Res.*, vol. 27, no. 17, pp. 2309–2317, Sep. 2012.
- [28] D. H. Kim, N. G. Cho, H. G. Kim, and W.-Y. Choi, "Structural and electrical properties of indium doped ZnO thin films fabricated by RF magnetron sputtering," *J. Electrochem. Soc.*, vol. 154, no. 11, p. H939, 2007.
- [29] P. Singh, R. Kumar, and R. K. Singh, "Progress on transition metal-doped ZnO nanoparticles and its application," *Ind. Eng. Chem. Res.*, vol. 58, no. 37, pp. 17130–17163, Sep. 2019.
- [30] M. A. Islam, M. S. Hossain, M. M. Aliyu, M. R. Karim, T. Razykov, K. Sopian, and N. Amin, "Effect of CdCl<sub>2</sub> treatment on structural and electronic property of CdTe thin films deposited by magnetron sputtering," *Thin Solid Films*, vol. 546, pp. 367–374, Nov. 2013.
- [31] M. A. Islam, M. U. Khandaker, and N. Amin, "Effect of deposition power in fabrication of highly efficient CdS: O/CdTe thin film solar cell by the magnetron sputtering technique," *Mater. Sci. Semicond. Process.*, vol. 40, pp. 90–98, Dec. 2015.
- [32] S. K. Suram, P. F. Newhouse, and J. M. Gregoire, "High throughput light absorber discovery, part 1: An algorithm for automated tauc analysis," *ACS Combinat. Sci.*, vol. 18, no. 11, pp. 673–681, Nov. 2016.
- [33] K. Satoh, Y. Kakehi, A. Okamoto, S. Murakami, F. Uratani, and T. Yotsuya, "Influence of oxygen flow ratio on properties of Zn<sub>2</sub>SnO<sub>4</sub> thin films deposited by RF magnetron sputtering," *Japanese J. Appl. Phys.*, vol. 44, no. L34, 2004.
- [34] S. Edinger, N. Bansal, M. Bauch, R. A. Wibowo, R. Hamid, G. Trimmel, and T. Dimopoulos, "Comparison of chemical bath-deposited ZnO films doped with Al, Ga and In," *J. Mater. Sci.*, vol. 52, no. 16, pp. 9410–9423, Aug. 2017.
- [35] M. A. Islam, K. S. Rahman, H. Misran, N. Asim, M. S. Hossain, M. Akhtaruzzaman, and N. Amin, "High mobility and transparent ZTO ETM prepared by RF reactive co-sputtering for perovskite solar cell application," *Results Phys.*, vol. 14, Sep. 2019, Art. no. 102518.
- [36] R. G. S. Pala and H. Metiu, "Modification of the oxidative power of ZnO(1010) surface by substituting some surface Zn atoms with other metals," *J. Phys. Chem. C*, vol. 111, no. 24, pp. 8617–8622, Jun. 2007.
- [37] P. F. Garcia, R. S. McLean, M. H. Reilly, and G. Nunes, "Transparent ZnO thin-film transistor fabricated by rf magnetron sputtering," *Appl. Phys. Lett.*, vol. 82, no. 7, pp. 1117–1119, Feb. 2003.
- [38] E. Rucavado, Q. Jeangros, D. F. Urban, J. Holovsky, Z. Remes, M. Duchamp, F. Landucci, R. E. Dunin-Borkowski, W. Körner, C. Elsässer, A. Hessler-Wyser, M. Morales-Masis, and C. Ballif, "Enhancing the optoelectronic properties of amorphous zinc tin oxide by subgap defect passivation: A theoretical and experimental demonstration," *Phys. Rev. B, Condens. Matter*, vol. 95, no. 24, Jun. 2017, Art. no. 245204.
- [39] M. A. Islam, T. Oshima, H. Matsuzaki, H. Nakahama, and Y. Ishikawa, "Carrier dynamics in the potential-induced degradation in single-crystalline silicon photovoltaic modules," *Jpn. J. Appl. Phys.*, vol. 57, Jul. 2018, Art. no. 08RG14.
- [40] S. Lie, J. M. Rui Tan, W. Li, S. W. Leow, Y. F. Tay, D. M. Bishop, O. Gunawan, and L. H. Wong, "Reducing the interfacial defect density of CZTSSe solar cells by Mn substitution," *J. Mater. Chem. A*, vol. 6, no. 4, pp. 1540–1550, 2018.
- [41] A. Bera, A. D. Sheikh, M. A. Haque, R. Bose, E. Alarousu, O. F. Mohammed, and T. Wu, "Fast crystallization and improved stability of perovskite solar cells with Zn<sub>2</sub>SnO<sub>4</sub> electron transporting layer: Interface matters," *ACS Appl. Mater. Interfaces*, vol. 7, pp. 8404–28411, Dec. 2015.



**MOHAMMAD AMINUL ISLAM** (Member, IEEE) received the M.Sc. (research) and Ph.D. degrees in electrical, electronic, and system engineering from Universiti Kebangsaan Malaysia (UKM), Malaysia, in 2012 and 2015, respectively. He has served several years in the Department of Electrical and Electronic Engineering as a Lecturer and an Assistant Professor at The International Islamic University Chittagong (IIUC), Bangladesh. He was a Postdoctoral Research Fellow with the Nara Institute of Science and Technology (NAIST), Nara, Japan, and with Universiti Tenaga Nasional (UNITEN), Putrajaya, Malaysia. He is currently serving as a Senior Lecturer with the University of Malaya, Kuala Lumpur, Malaysia. He is affiliated with the IEEE and IEEE young professionals and has organized and served as a technical committee for several IEEE conferences since 2013. His research interests include renewable energy resources, solar photovoltaic technologies, solar cells and PV systems, microelectronics, nanotechnology, and so on, with over 50 peer-reviewed publications.





**MD. KHAN SOBAYEL BIN RAFIQ** (Associate Member, IEEE) was born in Dhaka, Bangladesh. He received the B.Sc. degree in physics, in 2003, and completed his Advanced Engineering Course in military engineering, in 2006, the master's degree in energy & operational management from Staffordshire University, U.K., and the Ph.D. degree from The National University of Malaysia (UKM), Malaysia. He started his carrier in military since 2003 but thirst of acquiring knowledge

brought him in the field of scientific research. He is currently serving as a Postdoctoral Research Fellow with the Solar Energy Research Institute (SERI), The National University of Malaysia (UKM). His research interests include design and fabrication of thin film solar cell, perovskite solar cell, layer optimization in thin films, coating, renewable energy, and material physics, with over ten scientific publications. He is also a member of American Association for the Advancement of Science. He is also an Associate Member of IEEE Community. He received two national awards in his early days: for development of handy tools for military personnel and for contribution in National ID card project.



**HALINA MISRAN** has been serving as an Associate Professor with the Department of Mechanical Engineering, College of Engineering, Universiti Tenaga Nasional, since 2015. Previously, she had served as a Senior Lecturer at the Department of Mechanical Engineering for nine years, where she also led the Nanoarchitectonic research group specialising in nanomaterials and metal-organic framework (MOF) for environmental applications. She received the Mombukagakusho Scholarship

in 2000 to pursue her postgraduate studies from the Japanese Ministry of Education, Toyohashi University of Technology. Her research interests include green sol-gel, nanomaterials, gases adsorption, carbon capture and utilisation, and renewable metal-organic framework materials. She is actively promoting green synthesis techniques and awareness in producing nanostructured materials.



**MD. AKHTAR UZZAMAN** (Senior Member, IEEE) received the B.Sc. degree in applied chemistry and the M.Sc. degree in chemical engineering from the University of Dhaka, Bangladesh, in 1996 and 1998, respectively, and the Ph.D. degree from the Institute for Molecular Science (IMS), Okazaki, Japan, in March 2003. In 2000, he was awarded the Japanese Government's Mombukagakusho Scholarship and joined IMS, to pursue his Ph.D. degree. After his Ph.D., he joined

the Department of Electronic Chemistry, The Tokyo Institute of Technology, Japan, as a Postdoctoral Researcher for three years. Subsequently, he worked as a Chemist with Fujifilm Fine Chemical Company, Japan, from 2006 to 2007, as an Assistant Professor with King Saud University, Saudi Arabia, from 2009 to 2010, an Assistant Professor with the Department of Chemistry, Tohoku University, Sendai, Japan, from 2010 to 2012, and as a Senior Lecturer with the Department of Chemistry, University of Malaya, from 2012 to 2013. He is currently serving with the Solar Energy Research Institute (SERI), The National University of Malaysia (Universiti Kebangsaan Malaysia). He was awarded with one of the most prestigious fellowship of Japan Society for the Promotion Science (JSPS) from 2007 to 2009 at the Department of Electronics and Applied Physics, The Tokyo Institute of Technology. His research interests include rational design of organic/inorganic semiconductors, nano-materials for various applications, including dye-sensitized solar cells (DSSCs), perovskite thin-film solar cell, graphene /quantum dots-based hybrid solar cells, bulk-heterojunction solar cells (BHJs), light-emitting organic field-effect transistors (LE-OFETs), organic thin-film transistors (OTFTs), flexible memory devices, chemical and biological sensors, and nano-electronics and electroluminescence devices.



**KUAANAN TECHATO** received the Ph.D. degree in environmental management from Chulalongkorn University, Thailand. He is currently working as an Associate Professor with the Faculty of Environmental Management, Prince of Songkla University, Thailand. He is also acting as the Dean of the Faculty of Environmental Management, Prince of Songkla University. His research interests include renewable energy, environmental sciences, environmental management, energy and

environment policy, and green roof and wall. He has published numbers of research articles in national and international journals.



**GHULAM MUHAMMAD** (Senior Member, IEEE) received the Ph.D. degree in electrical and computer engineering from Toyohashi University and Technology, Japan, in 2006. He is currently a Professor with the Department of Computer Engineering, College of Computer and Information Sciences, King Saud University, Riyadh, Saudi Arabia. He has authored and coauthored more than 250 publications, including IEEE/ACM/Springer/Elsevier journals, and flag-

ship conference papers. He has two U.S. patents. His research interests include image and speech processing, machine learning, AI, and smart healthcare.



**NOWSHAD AMIN** is currently serving as a Strategic Hire Professor with the Institute of Sustainable Energy, The National Energy University (Universiti Tenaga Nasional), Malaysia. He is also an Adjunct Professor with The National University of Malaysia (Universiti Kebangsaan Malaysia). Previously, he has served 11 years in the Department of Electrical, Electronic & Systems Engineering, The National University of Malaysia (Universiti Kebangsaan Malaysia),

where he also led the Solar Photovoltaic Research Group under the Solar Energy Research Institute (SERI). He has also served as the Visiting Professor at the King Saud University of Saudi Arabia from 2010 till 2016. After completing the higher secondary education from his native country, Bangladesh, he received the Japanese Ministry of Education (MONBUSHO) Scholarship to pursue the diploma degree in electrical engineering from the Gunma National College of Technology in 1994, the bachelor' degree in electrical and electronic engineering from the Toyohashi University of Technology in 1996, and the master's and Ph.D. degrees in solar photovoltaic technology from The Tokyo Institute of Technology, in 1998 and 2001, respectively. He has served as the CTO of a University Spin-off company financed by the Malaysian Technology Development Center (MTDC). He has authored more than 350 peer-reviewed publications, a few books, and book chapters. He is actively involved in promoting renewable energy to the developing countries in South and South East Asia, and working as an enthusiastic promoter for the affordable renewable energy resources. His research interests include microelectronics, renewable energy, solar photovoltaic applications, and thin-film solar PV development. His research focuses on the commercialization of solar photovoltaic products from his patented entities.

...